THE ASTROPHYSICAL JOURNAL, 520:L79–L81, 1999 August 1

POLARIZATION OF THE Lyα HALOS AROUND SOURCES BEFORE COSMOLOGICAL REIONIZATION

GEORGE B. RYBICKI AND ABRAHAM LOEB
Harvard-Smithsonian Center for Astrophysics, 60 Garden Street, Cambridge, MA 02138
Received 1999 March 18; accepted 1999 May 25; published 1999 June 18

ABSTRACT

In Loeb & Rybicki (hereafter Paper I), it was shown that before reionization, the scattering of Lyα photons from a cosmological source might lead to a fairly compact ($\sim$15″) Lyα halo around the source. Observations of such halos could constrain the properties of the neutral intergalactic medium and, in particular, yield the cosmological density parameters of baryons and matter on scales where the Hubble flow is unperturbed. Paper I did not treat the polarization of this scattered radiation but did suggest that the degree of such polarization might be large. In this Letter, we report on improved calculations for these Lyα halos, now accounting for the polarization of the radiation field. The polarization is linear and is oriented tangentially to the projected displacement from the center of the source. The degree of polarization is found to be 14% at the core radius, where the intensity has fallen to half of the central value. It rises to 32% and 45% at the radii where the intensity has fallen to one-tenth and one-hundredth of the central intensity, respectively. At larger radii, the degree of polarization rises further, asymptotically to 60%. Such high values of polarization should be easily observable and provide a clear signature of the phenomenon of Lyα halos surrounding sources prior to reionization.

Subject headings: cosmology: theory — line: profiles

1. INTRODUCTION

At present, high-redshift galaxies are detected out to $z \lesssim 5.6$ and are found to be strong Lyα emitters (Dey et al. 1998; Hu, Cowie, & McMahon 1998; Spinrad et al. 1998; Weymann et al. 1998). Popular cosmological models predict that at somewhat higher redshifts, $z \sim 10$, the hydrogen in the intergalactic medium (IGM) was transformed from being predominantly neutral to being ionized because of the UV radiation emitted by the first stars and miniquasars (see, e.g., Gnedin & Ostriker 1997; Haiman & Loeb 1998, 1999). Prior to this epoch of reionization, the neutral IGM was highly opaque to resonant Lyα photons. Hence, the Lyα photons emitted by early galaxies were scattered in their vicinity by the surrounding IGM. In a previous paper (Loeb & Rybicki 1999, hereafter Paper I), we have shown that this intergalactic scattering results in compact ($\sim$15″) halos of Lyα light around such sources. The scattered photons compose a line of a universal shape, which is broadened and redshifted by $\sim 10^3$ km s^{-1} relative to the source. The detection of these intergalactic Lyα halos could provide a unique tool for probing the neutral IGM before and during the epoch of reionization. In addition, we have found that observations of the Lyα intensity profile on scales where the Hubble flow is only weakly perturbed could constrain the cosmological density parameters of baryons (Ω_b) and matter (Ω_M).

Paper I had suggested, but not demonstrated, that the scattered Lyα light would be highly polarized. The polarization signal is important in that it provides an unambiguous signature of the scattering nature of the diffuse Lyα halos around high-redshift galaxies. Due to the spherical symmetry of the scattering geometry, the linear polarization of the scattered radiation is expected to be oriented tangentially relative to the projected displacement from the center of the source.

In this Letter, we report on a detailed calculation of the polarization properties of scattered Lyα halos. In § 2 we describe the Monte Carlo approach employed in this calculation, and in § 3 we describe our numerical results. Finally, in § 4 we summarize the implications of these results.

2. POLARIZED MONTE CARLO METHOD

Let us first discuss the atomic scattering process for the Lyα line. We note that the hydrogen Lyα line at $\nu_0 = 2.466 \times 10^{15}$ Hz is actually a doublet consisting of the two fine-structure lines, $^2S_{1/2}$–$^2P^o_{1/2}$ and $^2S_{1/2}$–$^2P^o_{3/2}$, separated by 1.1×10^{10} Hz. Fortunately, as shown in Paper I, the regime of interest to us involves frequency shifts from these line centers on the order of $\nu_* \approx 10^{13}$ Hz, which are much larger than the separation of the lines. In this regime, quantum-mechanical interference between the two lines acts in such a way as to give a scattering behavior identical to that of a classical oscillator, i.e., the same as pure Rayleigh scattering (Stenflo 1980). (Using an incoherent superposition of the results of Hamilton 1947 for the two lines, one would incorrectly conclude that only one-third of the scattering is polarized.)

We shall now describe the modifications of the Monte Carlo method of Paper I that are necessary to treat polarization. Monte Carlo methods for polarized radiative transfer are often formulated using "photons" that are actually groups of photons with specified Stokes parameters (see, e.g., Whitney 1991; Code & Whitney 1995). However, for the present case, we found that a more convenient description of polarization was to use individual photons, each with a definite state of 100% linear polarization, a description previously used by Angel (1969). (There is no need to consider circular polarization here, since the central source is assumed to be unpolarized, and Rayleigh scattering cannot generate circular polarization, except from circular polarization.) If the direction of the photon is given by the unit vector $\boldsymbol{n}$, then its polarization is defined by a real unit vector $\boldsymbol{e}$, with $\boldsymbol{n} \cdot \boldsymbol{e} = 0$. In this formulation, the observed Stokes parameters result from the statistics of binning together multiple, independent photons.

With this description of photons, the polarized Monte Carlo method involves much the same steps as the unpolarized version of Paper I. One difference is in the handling of the polarized Rayleigh scattering process, which is done as follows: the angular distribution of the scattered photon has a probability distribution per solid angle proportional to $\sin^2 \Theta$, where Θ is the angle between the scattered photon and the polarization

vector of the incident photon. This is simulated using a rejection technique: we choose a random unit vector $\boldsymbol{n}'$ (uniform in solid angle) and a uniform random deviate R on (0, 1), and test whether $R < 1 - (\boldsymbol{e}\cdot\boldsymbol{n}')^2$; if not, we start again with new random choices for $\boldsymbol{n}'$ and R; the process is repeated until the test is passed, and then $\boldsymbol{n}'$ is taken as the new photon direction. The new polarization vector $\boldsymbol{e}'$ is determined by finding the normalized projection of the old polarization vector $\boldsymbol{e}$ onto the plane normal to $\boldsymbol{n}'$, i.e., $\boldsymbol{e}' = \boldsymbol{g}/|\boldsymbol{g}|$, where $\boldsymbol{g} = \boldsymbol{e} - (\boldsymbol{e}\cdot\boldsymbol{n}')\boldsymbol{n}'$. As in Paper I, an individual photon is followed through a number of scattering events until it escapes.

The only remaining question is how to characterize the polarization of the escaped, observed radiation in the plane of the sky as a function of impact parameter p. From symmetry, we know that this radiation can be characterized by the intensities parallel to the projected radius vector, I_l, and perpendicular to it, I_r. If χ is the angle between the photon's polarization vector and the projected radius vector, then it contributes to the appropriate histogram bins a fractional photon number $\cos^2\chi$ to I_l and $\sin^2\chi$ to I_r (these are the squares of the components of the polarization vector). With appropriate normalizations (see Paper I), these histograms determine the two intensities I_l and I_r. In terms of these, the degree of polarization is $\Pi = |I_l - I_r|/(I_l + I_r)$.

An alternative way of stating the results is in terms of the Stokes parameters I and Q, which are related to the above intensities by $I = I_l + I_r$ and $Q = I_l - I_r$. The degree of polarization is $\Pi = |Q|/I$. These Stokes parameters can also be found directly in the Monte Carlo method by binning with fractional photon number 1 for I and $\cos^2\chi - \sin^2\chi = \cos 2\chi$ for Q.

The above polarized Monte Carlo method was tested by solving the classical Milne problem for a Rayleigh scattering atmosphere (Chandrasekhar 1960, § 68). The results for the emergent intensities I_l and I_r agreed, to within statistical errors, with precise analytical results (Chandrasekhar 1960, Table XXIV, p. 248).

3. RESULTS

As in Paper I, we use rescaled variables (denoted by tildes), allowing one single solution to apply to all physical cases. In particular, we normalize frequencies by

$$\nu_\star = 5.6 \times 10^{12}\Omega_b h_0[\Omega_M(1+z_s)^{-3} + (1-\Omega_M-\Omega_\Lambda) \times (1+z_s)^{-4} + \Omega_\Lambda(1+z_s)^{-6}]^{-1/2}\ \mathrm{Hz} \quad (1)$$

and distances by

$$r_\star = \frac{6.7(\Omega_b/\Omega_M)\ \mathrm{Mpc}}{[1 + (1-\Omega_M-\Omega_\Lambda)\Omega_M^{-1}(1+z_s)^{-1} + (\Omega_\Lambda/\Omega_M)(1+z_s)^{-3}]}, \quad (2)$$

where Ω_b, Ω_M, and Ω_Λ are the density parameters of baryons, matter, and the vacuum, respectively; z_s is the source redshift; and h_0 is the Hubble constant in units of 100 km s^{-1} Mpc^{-1}. The radiation intensity is normalized by $I_\star = \dot{N}_\alpha/(r_\star^2\nu_\star)$, where $\dot{N}_\alpha$ is the steady emission rate of Lyα photons by the source.

The Monte Carlo method was used to follow the scattering of 10^8 photons, a sufficiently large number to provide reasonable statistical accuracy (except at very small impact parameters). The profile of the frequency-integrated total Stokes intensity $\tilde{I}$ versus impact parameter $\tilde{p}$ is given in Figure 1 (*upper solid curve*). The corresponding result from Paper I, in which the scattering was approximated as unpolarized and isotropic, is given as the dashed curve. The new curve is seen to be slightly more centrally concentrated, with a central intensity about 25% higher than that of Paper I.

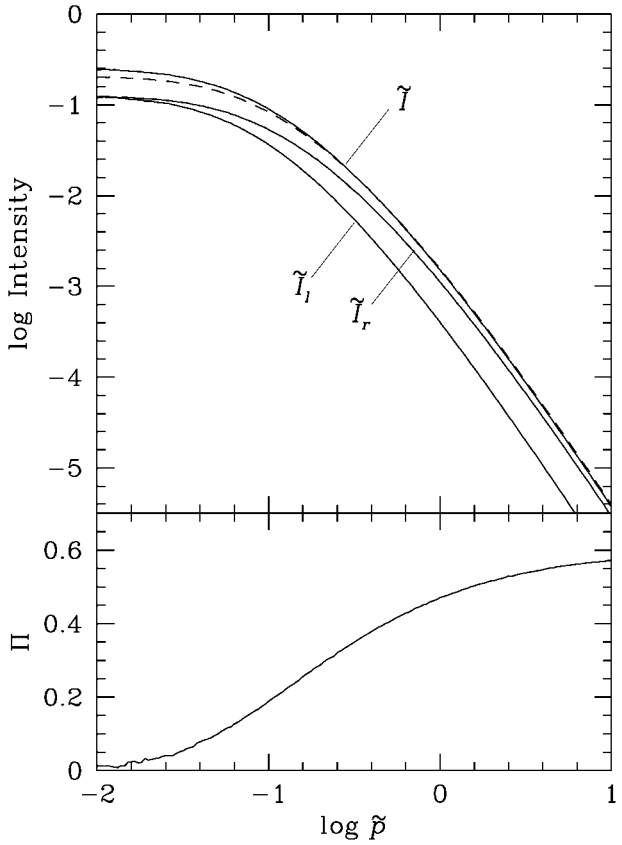

FIG. 1.—*Top*: The solid curves give the frequency-integrated intensities $\tilde{I}$, $\tilde{I}_l$, and $\tilde{I}_r$ vs. the impact parameter $\tilde{p}$. The dashed curve is the $\tilde{I}$ found in Paper I using isotropic, unpolarized scattering. *Bottom*: The degree of polarization Π vs. the impact parameter.

The "core" radius, where the total Stokes intensity $\tilde{I}$ has fallen to half its central value, is at $\tilde{p} = 0.070$. The radii where the intensity falls to one-tenth and one-hundredth of the central intensity are $\tilde{p} = 0.25$ and 0.80, respectively. At large impact parameters, $\tilde{I}$ falls approximately as $\tilde{p}^{-3}$.

The polarized intensities $\tilde{I}_l$ and $\tilde{I}_r$ are also plotted in Figure 1. At the center of the observed disk, $\tilde{p} = 0$, both of these intensities are equal to $\tilde{I}/2$ by symmetry. For all other values of the impact parameter, we note that $\tilde{I}_r$ exceeds $\tilde{I}_l$ everywhere, and asymptotically by a factor of 4. Thus, the radiation is strongly linearly polarized with orientation tangential to the projected radius vector.

The lower panel of Figure 1 shows the degree of polarization Π versus the impact parameter. This parameter rises monotonically from zero at $\tilde{p} = 0$ (as required by symmetry) to about 14% at the core radius, and to 32% and 45% at the one-tenth and one-hundredth intensity points, respectively. At still larger impact parameters, the polarization rises even further to an asymptotic value of 60%. However, since the intensities are falling so rapidly, polarizations of that asymptotic magnitude may not be detectable in practice.

Some heuristic insight into why these polarizations are so high can be found by a comparison with the problem of the

Rayleigh scattering of radiation from a point source surrounded by an optically thin scattering medium with a power-law density profile $N(r) \propto r^{-n}$, which was first treated by Schuster (1879) in the context of Thomson scattering in the solar corona. Schuster showed that the total intensity is a power law in the impact parameter, $I \propto p^{-(n+1)}$, and the degree of polarization is $(n + 1)/(n + 3)$. To relate the asymptotic results of our problem to those of the Schuster problem, we first note that the radiation at large impact parameters is dominated by the scattering of photons that have taken one very large step from much nearer the source, so they are traveling almost radially, as they would from a point source. The second observation is that the Schuster result really applies more generally to a power-law dependence of the product of the scattering cross section $\sigma(r)$ times the density of the form $\sigma(r)N(r) \propto r^{-n}$. This is because only the optical depth along the radial direction is relevant to Schuster's derivation. In the situation treated by Schuster, the scattering cross section was constant. In our case, the density is constant, but the scattering cross section seen by these radial photons decreases inversely as the square of the distance, since the frequency displacement is redshifting linearly with distance, and the line profile varies inversely as the square of the frequency. Therefore, we should compare with the Schuster results for $n = 2$. This gives an inverse third power behavior for the intensity and $3/5 = 60\%$ for the degree of polarization, exactly as seen in our asymptotic results.

The image of the halo taken in unpolarized light will have circular symmetry on the sky. A contour plot of such an image is shown in Figure 2*a*. The 10 contours are spaced by 0.5 mag (0.2 dex), so that the outer contour represents an intensity 10^{-2} times the central intensity.

These contours are distorted when the image is taken through a linear polarizing filter. Let us use a Cartesian coordinate system $(\tilde{p}_x, \tilde{p}_y)$ in the plane of the sky and assume the polarizing filter is oriented along the $\tilde{p}_y$ axis. At each point in the image, the observed intensity is given as a weighted average of the two intensities $\tilde{I}_l$ and $\tilde{I}_r$, namely,

$$\tilde{I}(\tilde{p}_x, \tilde{p}_y) = \tilde{I}_l \sin^2\theta + \tilde{I}_r \cos^2\theta, \tag{3}$$

where θ is the polar angle of the point relative to the $\tilde{p}_x$ axis, so that $\cos\theta = \tilde{p}_x/\tilde{p}$ and $\sin\theta = \tilde{p}_y/\tilde{p}$. Using this equation, the contours of the halo were constructed and are shown in Figure 2*b*, again using a separation of 0.5 mag between the contours. The distortions are very evident, even for the innermost contours.

The detectability of Lyα halos around high-redshift galaxies was discussed in detail in Paper I. We have found that although difficult, detection of halos at $z_s \lesssim 10$ might be feasible from space. For example, given the upper limit on the cosmic infrared background derived by *COBE* at 1.25 μm (Hauser et al. 1998), one could achieve a signal-to-noise ratio S/N = 10 after 10 hr of integration on an 8 m space telescope (such as the *Next Generation Space Telescope*) for sources at $z_s \sim 10$ that possess a Lya luminosity higher by an order of magnitude than the galaxy discovered by Dey et al. (1998). Such sources emit $\dot{N}_\alpha = 6 \times 10^{54}$ s^{-1} and might be found in wide-field surveys, based on the broad number-flux distribution that is predicted for high-redshift galaxies (see Fig. 2 in Haiman & Loeb 1999).

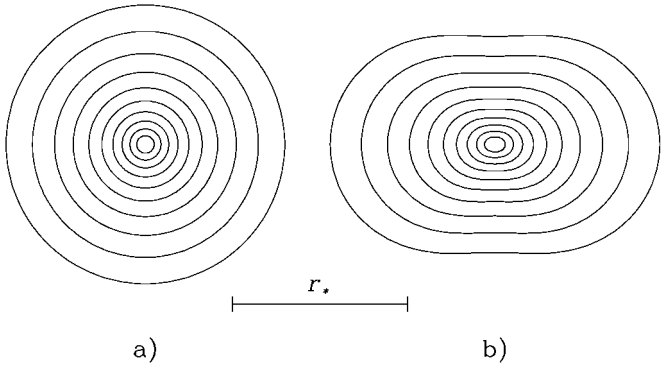

FIG. 2.—Predicted images of the Lyα halo in the plane of the sky, (*a*) as seen in total light and (*b*) as seen through a linear polarizing filter oriented vertically. The contours are separated by 0.5 mag, starting with the central intensity.

4. CONCLUSIONS

As shown in Paper I, the special type of Lyα halos associated with sources surrounded by the neutral IGM in a Hubble flow before reionization can be clearly characterized by their light profile and spectrum, which have a universal character. In this Letter, we have shown additionally that the polarizations associated with these Lyα halos are quite large, on the of order tens of percent, and have a particular universal behavior as a function of the impact parameter.

The polarization properties illustrated in Figure 1 could potentially be of importance in providing a critical test for distinguishing between Lyα halos of the type considered here as opposed to halos due to some other cause. In addition, the polarization signature can improve the S/N in separating faint Lyα halos from an unpolarized background light.

This work was supported in part by the NASA grants NAG5-7768 and NAG5-7039 (for A. L.). The authors gratefully acknowledge helpful conversations with Alex Dalgarno and Kenneth Wood.

REFERENCES

Angel, J. R. P. 1969, ApJ, 158, 219
Chandrasekhar, S. 1960, Radiative Transfer (New York: Dover)
Code, A. D., & Whitney, B. A. 1995, ApJ, 441, 400
Dey, A., Spinrad, H., Stern, D., Graham, J. R., & Chaffee, F. H. 1998, ApJ, 498, L93
Gnedin, N., & Ostriker, J. P. 1997, ApJ, 486, 581
Haiman, Z., & Loeb, A. 1998, ApJ, 503, 505
———. 1999, in After the Dark Ages: When Galaxies Were Young (the Universe at $2 < z < 5$), ed. S. S. Holt & E. P. Smith (Woodbury: AIP), 34
Hamilton, D. R. 1947, ApJ, 106, 457
Hauser, M. G., et al. 1998, ApJ, 508, 25
Hu, E. M., Cowie, L. L., & McMahon, R. G. 1998, ApJ, 502, L99
Loeb, A., & Rybicki, G. B. 1999, ApJ, in press (astro-ph/9902180) (Paper I)
Schuster, A. 1879, MNRAS, 40, 35
Spinrad, H., et al. 1998, AJ, 116, 2617
Stenflo, J. O. 1980, A&A, 84, 68
Weymann, R. J., et al. 1998, ApJ, 505, L95
Whitney, B. A. 1991, ApJS, 75, 1293